LETTER

doi:10.1038/nature10972

Systematic variation of the stellar initial mass function in early-type galaxies

Michele Cappellari[1], Richard M. McDermid[2], Katherine Alatalo[3], Leo Blitz[3], Maxime Bois[4], Frédéric Bournaud[5], M. Bureau[1], Alison F. Crocker[6], Roger L. Davies[1], Timothy A. Davis[1,7], P. T. de Zeeuw[7,8], Pierre-Alain Duc[5], Eric Emsellem[7,9], Sadegh Khochfar[10], Davor Krajnović[7], Harald Kuntschner[7], Pierre-Yves Lablanche[7,9], Raffaella Morganti[11,12], Thorsten Naab[13], Tom Oosterloo[11,12], Marc Sarzi[14], Nicholas Scott[1,15], Paolo Serra[11], Anne-Marie Weijmans[16] & Lisa M. Young[17]

Much of our knowledge of galaxies comes from analysing the radiation emitted by their stars, which depends on the present number of each type of star in the galaxy. The present number depends on the stellar initial mass function (IMF), which describes the distribution of stellar masses when the population formed, and knowledge of it is critical to almost every aspect of galaxy evolution. More than 50 years after the first IMF determination[1], no consensus has emerged on whether it is universal among different types of galaxies[2]. Previous studies indicated that the IMF and the dark matter fraction in galaxy centres cannot both be universal[3–7], but they could not convincingly discriminate between the two possibilities. Only recently were indications found that massive elliptical galaxies may not have the same IMF as the Milky Way[8]. Here we report a study of the two-dimensional stellar kinematics for the large representative ATLAS^{3D} sample[9] of nearby early-type galaxies spanning two orders of magnitude in stellar mass, using detailed dynamical models. We find a strong systematic variation in IMF in early-type galaxies as a function of their stellar mass-to-light ratios, producing differences of a factor of up to three in galactic stellar mass. This implies that a galaxy's IMF depends intimately on the galaxy's formation history.

As part of the ATLAS^{3D} project[9], we obtained integral-field maps of stellar kinematics for a volume-limited sample of 260 early-type (elliptical and lenticular) galaxies. They were selected to be closer than 42 Mpc to Earth and to have K_s-band total magnitudes of $M_K < -21.5$ mag (corresponding to galaxy stellar masses of $M \gtrsim 6 \times 10^9 M_\odot$, where $M_\odot$ is the solar mass), as determined from the Two Micron All Sky Survey at our adopted distances. Homogeneous imaging for all the galaxies in the r band was obtained in major part from data release 8 of the Sloan Digital Sky Survey and completed with our own photometry.

For all galaxies, we constructed six sets of dynamical models[10], which include an axisymmetric stellar component and a spherical dark halo, and fit the details of both the projected stellar distribution[11] and the two-dimensional stellar kinematics[9] (Fig. 1). Although the shape of the stellar component can be inferred directly from the galaxy images, the dark halo shape must be a free parameter of the models. Using the models, we explored a variety of plausible assumptions for the halo to test how these can affect our result. Our halo models include as limiting cases a maximum-ignorance model, where the halo parameters are directly fitted to the stellar kinematics, and some completely fixed models, where the halo follows the predictions of numerical simulations[12–14]. A detailed description of the model parameters is provided in Table 1. The key parameter we extract from all the models is the ratio, $(M/L)_{\rm stars}$, between the mass of the stellar component and the luminosity (in the r band). As illustrated in Fig. 1, the availability of integral-field data is the key to separating the stellar mass accurately from the possible dark matter using dynamical models and hence determining $(M/L)_{\rm stars}$. In fact, changes in $(M/L)_{\rm stars}$ at the level expected to result from IMF variations cause drastic changes to the quality of the model fits.

We also measured the $(M/L)_{\rm pop}$ ratio (in the r band) of the stellar population by fitting[15] the observed spectra using a linear combination of single stellar population synthetic spectra[16] of different ages (t) and metallicities ($[M/H]$), adopting for reference a Salpeter[1] IMF ($\xi(m) \propto m^x = m^{-2.3}$, where m is the stellar mass). The models use standard lower and upper mass cut-offs for the IMF of $0.1M_\odot$ and $100M_\odot$, respectively. We used linear regularization to reduce noise and produce smooth $M(t, [M/H])$ solutions consistent with the observations. The resulting $(M/L)_{\rm pop}$ ratio is that of the composite stellar population, and excludes the gas lost during stellar evolution. If all this gas were retained in the galaxies in gaseous form, it would systematically increase $(M/L)_{\rm pop}$ by about 30% (ref. 17). However, most of it is probably recycled into stars or expelled to larger radii. Although the measured trends have smaller scatter when using our full-spectrum fitting approach[15], similar conclusions are reached when the galaxies are approximated as one single stellar population, or when $(M/L)_{\rm pop}$ is computed using different population codes[16–18] and with a more traditional approach, which only focuses on the strength of a few stellar absorption spectral lines. Systematic offsets of about 10% in $(M/L)_{\rm pop}$ exist between the predictions of different population models for an identical set of assumed population parameters. The model that we use lies in the middle of this range. This sets the uncertainty in the absolute normalization of our plots. The random errors resulting from our population code[16] were estimated by applying the same spectral fitting approach to our integral-field spectroscopy data and to independent spectra obtained for a subset of 57 of our galaxies by the Sloan Digital Sky Survey. We inferred a root mean squared scatter of 12% in each individual $(M/L)_{\rm pop}$ determination.

The ratio between the dynamically derived $(M/L)_{\rm stars}$ values and the population-derived $(M/L)_{\rm Salp}$ values, calculated using a fixed Salpeter IMF, is shown in Fig. 2 as a function of $(M/L)_{\rm stars}$. We compare the observed ratio with the expected one if the galaxy had the 'light'

[1]Sub-department of Astrophysics, Department of Physics, University of Oxford, Denys Wilkinson Building, Keble Road, Oxford OX1 3RH, UK. [2]Gemini Observatory, Northern Operations Centre, 670 North A'ohoku Place, Hilo, Hawaii 96720, USA. [3]Department of Astronomy, Campbell Hall, University of California, Berkeley, California 94720, USA. [4]Observatoire de Paris, LERMA and CNRS, 61 Avenue de l'Observatoire, F-75014 Paris, France. [5]Laboratoire AIM Paris-Saclay, CEA/IRFU/SAp CNRS Université Paris Diderot, 91191 Gif-sur-Yvette Cedex, France. [6]Department of Astrophysics, University of Massachusetts, 710 North Pleasant Street, Amherst, Massachusetts 01003, USA. [7]European Southern Observatory, Karl-Schwarzschild-Strasse 2, 85748 Garching, Germany. [8]Sterrewacht Leiden, Leiden University, Postbus 9513, 2300 RA Leiden, The Netherlands. [9]Université Lyon 1, Observatoire de Lyon, Centre de Recherche Astrophysique de Lyon and Ecole Normale Supérieure de Lyon, 9 avenue Charles André, F-69230 Saint-Genis Laval, France. [10]Max-Planck Institut für extraterrestrische Physik, PO Box 1312, D-85478 Garching, Germany. [11]Netherlands Institute for Radio Astronomy, Postbus 2, 7990 AA Dwingeloo, The Netherlands. [12]Kapteyn Astronomical Institute, University of Groningen, Postbus 800, 9700 AV Groningen, The Netherlands. [13]Max-Planck Institut für Astrophysik, Karl-Schwarzschild-Strasse 1, 85741 Garching, Germany. [14]Centre for Astrophysics Research, University of Hertfordshire, Hatfield AL1 9AB, UK. [15]Centre for Astrophysics & Supercomputing, Swinburne University of Technology, PO Box 218, Hawthorn, Victoria 3122, Australia. [16]Dunlap Institute for Astronomy & Astrophysics, University of Toronto, 50 St George Street, Toronto, Ontario M5S 3H4, Canada. [17]Physics Department, New Mexico Institute of Mining and Technology, Socorro, New Mexico 87801, USA.

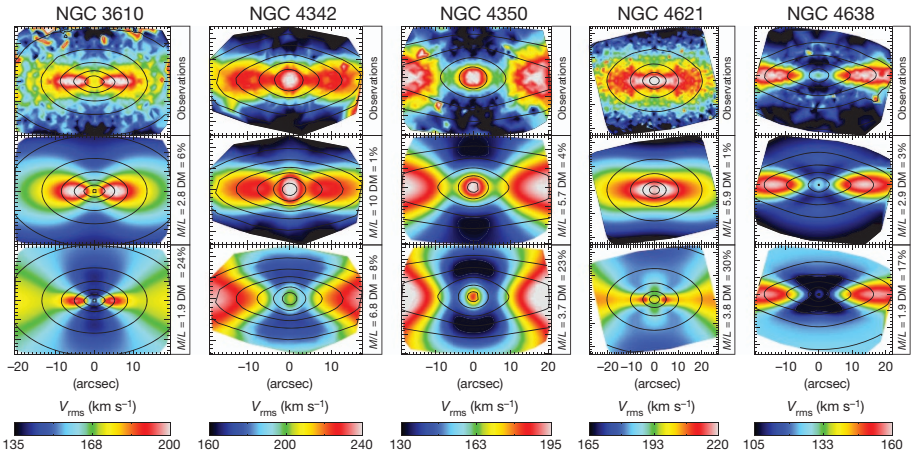

Figure 1 | Differentiating between the stellar and dark matter with integral-field stellar kinematics. The top row shows the symmetrized SAURON stellar kinematics ($V_{\rm rms} = \sqrt{V^2 + \sigma^2}$) as a function of spatial position on the sky for the five named galaxies, which represent a variety of shapes of the kinematics field and span a range of $(M/L)_{\rm stars}$ values. Here V is the mean stellar velocity and σ is the stellar velocity dispersion. The middle row shows the results of the best-fitting dynamical model[10] with a standard[12] dark halo (model B in Table 1). The bottom row shows the results of a dynamical model where the $(M/L)_{\rm stars}$ ratio was fixed to be 0.65 times the best-fitting one. This decrease in $(M/L)_{\rm stars}$ represents the change in stellar mass between a Salpeter IMF and a Kroupa IMF. The other three model parameters, the galaxy inclination (i), the orbital anisotropy (β_z) and the halo total mass (M_{200}), were optimized to fit the data, but cannot provide an acceptable description of the observations. The plots show that, for a standard halo profile, the data tightly constrain both the dark matter fraction and $(M/L)_{\rm stars}$. The constraint would be even stronger if we had assumed a more shallow inner-halo profile. The contours show the observed (top row) and modelled (middle and bottom rows) surface brightnesses. The $(M/L)_{\rm stars}$ ratio (M/L) and the fraction of dark matter (DM) within a sphere with radius equal to the projected half-light radius are printed next to each panel.

Kroupa[19] or Chabrier[20] IMFs, which are similarly deficient in low-mass stars; with the 'standard' Salpeter IMF, which is described by a simple power law in stellar mass (m) with exponent $x = -2.3$; and with two additional 'heavy' power-law IMFs with $x = -2.8$ and $x = -1.5$, respectively. The last two IMFs predict the same $(M/L)_{\rm pop}$ ratio. However, whereas for $x = -2.8$ the stellar population is dominated by dwarf stars, for $x = -1.5$ the large $(M/L)_{\rm pop}$ ratio is due to stellar remnants: black holes, neutron stars and white dwarfs. The dynamical mass measurements do not constrain the shape of the IMF directly, but only the overall mass normalization, and for this reason do not distinguish between the two cases.

The results from all sets of dynamical models are consistent with a similar systematic variation in the IMF normalization, by a factor of up to three in galaxy stellar mass. A clear trend is visible in particular for the most general of our set of models (Fig. 2d), which makes virtually no assumptions about halo shape but fits it directly to the data. However, similar trends are visible for all our plausible assumptions for the dark halo mass and profile as predicted by numerical simulations. This shows that, although the relative amplitude of the IMF variation does not depend on the correctness of the assumed halo model, it is entirely consistent with standard model predictions for the halo. As $(M/L)_{\rm stars}$ increases, the normalization of the inferred IMF varies from that of Kroupa and Chabrier to one more massive than the Salpeter IMF. The trend in IMF is still clearly visible in the subset of the 60 galaxies outside the Virgo galaxy cluster that have the most accurate distances and the best models fits. This shows that the trend cannot be due to biases in the models or distances, or to effects related to the cluster environment. The knee in the relation at $(M/L)_{\rm stars} \approx 6$ (r band) shows that the lowest $(M/L)_{\rm stars}$ values mainly reflect the age and metallicity of the population (with younger ages or lower metallicities decreasing $(M/L)_{\rm pop}$), and that the largest $(M/L)_{\rm stars}$ values mainly reflect the population's dwarf- or remnants-dominated IMF. The models with contracted halos show the same IMF trend and relative amplitude as the other models. However, contracted halos predict too little stellar mass for many of the galaxies with low $(M/L)_{\rm stars}$ ratios, even for the lightest Kroupa–Chabrier IMF. This suggests that contraction may not happen in most real galaxies, in agreement with recent numerical simulations that include a realistic treatment of baryon physics[21].

The trend in IMF reported here reconciles a number of apparently contradictory results on the normalization of the IMF that have accumulated in the past decade. The Kroupa–Chabrier-like normalization at low values of $(M/L)_{\rm stars}$ agrees with the one inferred for spiral galaxies[22]. The ATLAS$^{\rm 3D}$ project discovered that early-type galaxies with the lowest $(M/L)_{\rm pop}$ ratios resemble spiral galaxies with their gas removed[23], implying that these galaxies should have similar IMFs. The Kroupa–Chabrier normalization is also consistent with previous findings that this normalization is required if the stellar mass of early-type galaxies as a class is not to be overpredicted[3,24,25]. A Salpeter normalization at larger $(M/L)_{\rm stars}$ ratios is consistent on average

Table 1 | The axisymmetric dynamical models

Model	Description of the model	Fitted model parameters
A (Fig. 2a)	Galaxy model in which the total mass traces the observed galaxy light distribution. Any dark matter, if present, follows the stellar distribution.	i, β_z, $(M/L)_{\rm total}$
B (Fig. 2b)	Galaxy stellar component embedded in a spherical standard dark matter halo[12] with inner density $\rho(r) \propto r^{-1}$ for radii $r \ll r_{\rm s}$ and outer density $\rho(r) \propto r^{-3}$ for $r \gg r_{\rm s}$. The halo total mass, M_{200}, is fitted, and $r_{\rm s}$ is uniquely specified[13] by M_{200}.	i, β_z, $(M/L)_{\rm stars}$, M_{200}
C (Fig. 2c)	Model with a standard[12] halo contracted[14] according to the observed galaxy stellar density. The halo mass is fitted, and $r_{\rm s}$ is specified[13] by M_{200}.	i, β_z, $(M/L)_{\rm stars}$, M_{200}
D (Fig. 2d)	Model with a general halo inner density $\rho(r) \propto r^{\gamma}$ with fitted slope ($-1.6 < \gamma < 0$) and fitted total mass. The outer density becomes $\rho(r) \propto r^{-3}$, as in the standard halo[12], at radii $r \gg r_{\rm s} = 20$ kpc.	i, β_z, $(M/L)_{\rm stars}$, γ, M_{200}
E (Fig. 2e)	Model with a fixed standard halo[12]. M_{200} is specified[30] by the measured galaxy stellar mass and $r_{\rm s}$ is specified[13] by M_{200}.	i, β_z, $(M/L)_{\rm stars}$
F (Fig. 2f)	Model with a fixed standard halo[12] contracted[14] according to the observed galaxy stellar density. M_{200} is specified[30] by the measured galaxy stellar mass and $r_{\rm s}$ is specified[13] by M_{200}.	i, β_z, $(M/L)_{\rm stars}$

$(M/L)_{\rm total}$ is the ratio between the galaxy total mass and the corresponding luminosity in the r band and $r_{\rm s}$ is the break radius of the halo, between the two power-law regimes. In model D, the steepest slope, $\gamma = -1.6$, is the extreme measured value for any of the contracted models C. The adopted break radius, $r_{\rm s} = 20$ kpc, is the median value for all models E. However, this choice is unimportant because the fits are almost insensitive to the shape of the dark halo profile outside the much smaller radii where kinematics is available. The same values of $(M/L)_{\rm stars}$ are obtained with a pure power-law halo.

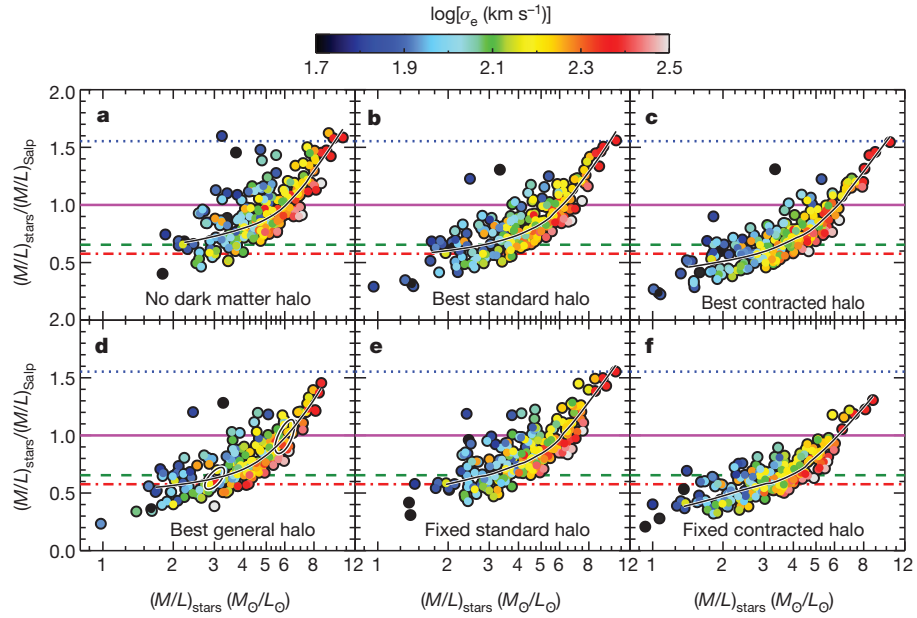

Figure 2 | Systematic variation of the IMF in early-type galaxies. Ratio between the $(M/L)_{stars}$ values of the stellar component, determined using dynamical models, and the $(M/L)_{Salp}$ values of the stellar population, measured using stellar population models with a Salpeter IMF, as a function of $(M/L)_{stars}$. The black solid line is a locally weighted scatterplot smoothed version of the data. Colours indicate the galaxies' stellar velocity dispersion (σ_e), which is related to galaxy mass. The horizontal lines indicate the expected values for the ratio if the galaxy had (i) a Chabrier IMF (red dash–dot line); (ii) a Kroupa IMF (green dashed line); (iii) a Salpeter IMF ($x = -2.3$, solid magenta line) or one of two additional power-law IMFs with (iv) $x = -2.8$ and (v) $x = -1.5$ (blue dotted line). The different panels correspond to different assumptions for the dark matter halos used in the dynamical models: details are given in Table 1. A clear curved relation is visible in all panels. Panels **a**, **b** and **e** look quite similar, as for all of them the dark matter contributes only a small fraction (zero in **a** and a median of 12% in **b** and **e**) of the total mass inside a sphere with the projected size of the region where we have kinematics (about one projected half-light radius). Panel **f**, with a fixed contracted halo, still shows the same IMF variation, but is almost systematically lower in $(M/L)_{stars}$ by 35%, reflecting the increase in dark matter fraction. The two ellipses plotted over the smooth relation in **d** show the representative 1σ errors for one measurement at the given locations. We excluded from the plot the galaxies with a very young stellar population (selected as having an Hβ absorption line strength >2.3 Å). These galaxies have strong radial gradients in their populations, which violates our assumption that all our various M/L values are spatially constant and makes both $(M/L)_{Salp}$ and $(M/L)_{stars}$ inaccurate.

with results from strong gravitational lensing[5], which are restricted to the galaxies with the largest velocity dispersions ($\sigma \gtrsim 200\,km\,s^{-1}$). Finally, that some large-$(M/L)_{stars}$ galaxies have IMF normalizations more massive than the Salpeter normalization is broadly consistent with the finding from the depths of spectral features of eight massive galaxies[8] which indicate that they must be dominated by a population of dwarf stars.

If instead the largest $(M/L)_{pop}$ ratios were due to stellar remnants, our results would be consistent with indirect arguments based on the relation between the colour of a stellar population and its fraction of ionizing photons, suggesting an IMF slope that becomes flatter for more massive, star-forming galaxies[26,27]. However, our result is difficult to compare with this result directly, owing to the large difference in the sample selections. Moreover, these studies[26,27] measure the instantaneous IMF, when the stars are forming, whereas all previous studies we mentioned, and the one in this Letter, measure the 'integrated' galaxy IMF resulting from the cumulative history of star formation[28] and evolutionary mechanisms that the galaxy has experienced.

The discovered trend in IMF is also consistent with previous findings that the total M/L ratio in the centre of galaxies varies by a factor of at least two more than would be expected for a stellar population with constant dark matter fraction and a universal IMF[3]. Various previous attempts could not distinguish whether the mass discrepancy was due to non-universality of dark matter or that of IMF[4–7,29]. The studies were limited either by small samples or non-optimal data[3,6], or used simplified galaxy models that could bias the quantitative interpretation of the results[4,5,7,29]. We resolve both of these issues in this Letter.

Our study demonstrates that the assumption of a universal IMF, which is made in nearly every aspect of galactic astrophysics, stellar populations and cosmology, is inconsistent with real galaxies. Our results pose a challenge to galaxy formation models, which will have to explain how stars 'know' what kind of galaxy they will end up inside. A possible explanation would be for the IMF to depend on the prevailing physical conditions when the galaxy formed the bulk of its stars. Although galaxies merge hierarchically, there is growing evidence that present-day, massive, early-type galaxies formed most of their stars in more-intense starbursts and at higher redshifts than spiral galaxies. This could lead to the observed difference in IMF. Unfortunately, there is no consensus among the theoretical models for how the IMF should vary with physical conditions. A new generation of theoretical and observational studies will have to provide insight into which physical mechanisms are responsible for the systematic IMF variation we find.

Received 13 December 2011; accepted 13 February 2012.

1. Salpeter, E. E. The luminosity function and stellar evolution. *Astrophys. J.* **121,** 161–167 (1955).
2. Bastian, N. Covey, K. R. & Meyer, M. R. A universal stellar initial mass function? A critical look at variations. *Annu. Rev. Astron. Astrophys.* **48,** 339–389 (2010).
3. Cappellari, M. *et al.* The SAURON project – IV. The mass-to-light ratio, the virial mass estimator and the fundamental plane of elliptical and lenticular galaxies. *Mon. Not. R. Astron. Soc.* **366,** 1126–1150 (2006).
4. Tortora, C., Napolitano, N. R., Romanowsky, A. J., Capaccioli, M. & Covone, G. Central mass-to-light ratios and dark matter fractions in early-type galaxies. *Mon. Not. R. Astron. Soc.* **396,** 1132–1150 (2009).
5. Treu, T. *et al.* The initial mass function of early-type galaxies. *Astrophys. J.* **709,** 1195–1202 (2010).
6. Thomas, J. *et al.* Dynamical masses of early-type galaxies: a comparison to lensing results and implications for the stellar initial mass function and the distribution of dark matter. *Mon. Not. R. Astron. Soc.* **415,** 545–562 (2011).
7. Dutton, A. A. *et al.* Dark halo response and the stellar initial mass function in early-type and late-type galaxies. *Mon. Not. R. Astron. Soc.* **416,** 322–345 (2011).
8. van Dokkum, P. G. & Conroy, C. A substantial population of low-mass stars in luminous elliptical galaxies. *Nature* **468,** 940–942 (2010).
9. Cappellari, M. *et al.* The ATLAS^{3D} project – I. A volume-limited sample of 260 nearby early-type galaxies: science goals and selection criteria. *Mon. Not. R. Astron. Soc.* **413,** 813–836 (2011).

10. Cappellari, M. Measuring the inclination and mass-to-light ratio of axisymmetric galaxies via anisotropic Jeans models of stellar kinematics. *Mon. Not. R. Astron. Soc.* **390,** 71–86 (2008).
11. Emsellem, E., Monnet, G. & Bacon, R. The multi-gaussian expansion method: a tool for building realistic photometric and kinematical models of stellar systems I. The formalism. *Astron. Astrophys.* **285,** 723–738 (1994).
12. Navarro, J. F., Frenk, C. S. & White, S. D. M. The structure of cold dark matter halos. *Astrophys. J.* **462,** 563–575 (1996).
13. Klypin, A. A., Trujillo-Gomez, S. & Primack, J. Dark matter halos in the standard cosmological model: results from the Bolshoi simulation. *Astrophys. J.* **740,** 102 (2011).
14. Gnedin, O. Y. *et al.* Halo contraction effect in hydrodynamic simulations of galaxy formation. Preprint at ⟨http://arxiv.org/abs/1108.5736⟩ (2011).
15. Cappellari, M. & Emsellem, E. Parametric recovery of line-of-sight velocity distributions from absorption-line spectra of galaxies via penalized likelihood. *Publ. Astron. Soc. Pacif.* **116,** 138–147 (2004).
16. Vazdekis, A. *et al.* Evolutionary stellar population synthesis with MILES - I. The base models and a new line index system. *Mon. Not. R. Astron. Soc.* **404,** 1639–1671 (2010).
17. Maraston, C. Evolutionary population synthesis: models, analysis of the ingredients and application to high-*z* galaxies. *Mon. Not. R. Astron. Soc.* **362,** 799–825 (2005).
18. Bruzual, G. & Charlot, S. Stellar population synthesis at the resolution of 2003. *Mon. Not. R. Astron. Soc.* **344,** 1000–1028 (2003).
19. Kroupa, P. On the variation of the initial mass function. *Mon. Not. R. Astron. Soc.* **322,** 231–246 (2001).
20. Chabrier, G. Galactic stellar and substellar initial mass function. *Publ. Astron. Soc. Pacif.* **115,** 763–795 (2003).
21. Duffy, A. R. *et al.* Impact of baryon physics on dark matter structures: a detailed simulation study of halo density profiles. *Mon. Not. R. Astron. Soc.* **405,** 2161–2178 (2010).
22. Bell, E. F. & de Jong, R. S. Stellar mass-to-light ratios and the Tully-Fisher relation. *Astrophys. J.* **550,** 212–229 (2001).
23. Cappellari, M. *et al.* The ATLAS^{3D} project – VII. A new look at the morphology of nearby galaxies: the kinematic morphology-density relation. *Mon. Not. R. Astron. Soc.* **416,** 1680–1696 (2011).
24. Renzini, A. in *The Initial Mass Function 50 Years Later* (ed. Corbelli, E., Palla, F. and Zinnecker, H.) 221 (Springer, 2005).
25. Ferreras, I., Saha, P. & Burles, S. Unveiling dark haloes in lensing galaxies. *Mon. Not. R. Astron. Soc.* **383,** 857–863 (2008).
26. Hoversten, E. A. & Glazebrook, K. Evidence for a nonuniversal stellar initial mass function from the integrated properties of SDSS galaxies. *Astrophys. J.* **675,** 163–187 (2008).
27. Gunawardhana, M. L. P. *et al.* Galaxy and mass assembly (GAMA): the star formation rate dependence of the stellar initial mass function. *Mon. Not. R. Astron. Soc.* **415,** 1647–1662 (2011).
28. Kroupa, P. & Weidner, C. Galactic-field initial mass functions of massive stars. *Astrophys. J.* **598,** 1076–1078 (2003).
29. Deason, A. J., Belokurov, V., Evans, N. W. & McCarthy, I. G. Elliptical galaxy masses out to five effective radii: the realm of dark matter. *Astrophys. J.* **748,** 2 (2012).
30. Moster, B. P. *et al.* Constraints on the relationship between stellar mass and halo mass at low and high redshift. *Astrophys. J.* **710,** 903–923 (2010).

Acknowledgements M.C. acknowledges support from a Royal Society University Research Fellowship. This work was supported by the rolling grants 'Astrophysics at Oxford' from the UK Research Councils. R.L.D. acknowledges support from Christ Church College, Oxford University, and from the Royal Society in the form of a Wolfson Merit Award. S.K. acknowledges support from the Royal Society Joint Projects Grant. R.M.M. is supported by the Gemini Observatory. T.N. and M. Bois acknowledge support from the DFG Cluster of Excellence 'Origin and Structure of the Universe'. M.S. acknowledges support from a STFC Advanced Fellowship. N.S. and T.A.D. acknowledge support from an STFC studentship.

Author Contributions All authors contributed extensively to the work presented in this paper.

Author Information Reprints and permissions information is available at www.nature.com/reprints. The authors declare no competing financial interests. Readers are welcome to comment on the online version of this article at www.nature.com/nature. Correspondence and requests for materials should be addressed to M.C. (cappellari@astro.ox.ac.uk).